57

Thermal behaviour of QCD

57.1 The QCD phases

We study here the uses of QCD spectral sum rules (QSSR) in a matter with non-zero temperature T and non-zero chemical potential μ (so-called Quark-Gluon Plasma (QGP)). Since the corresponding critical temperature for the *colour deconfinement* is expected to be rather small ($T_c \leq 1$ GeV), these new states of matter can be investigated in high-energy hadron collisions. At high enough temperature $T \geq T_c \approx 150 - 200$ MeV corresponding to a vacuum pressure of about 500 MeV/fm^3, QGP phase occurs and can be understood without confinement. In this phase, one also expects that chiral symmetry is restored (*chiral symmetry restoration*). However, it is a priori unclear, if the QGP phase and the chiral symmetry restoration occurs at the same temperature or not. Untuitively, one can expect that the deconfinement phase occurs before the chiral symmetry restoration. An attempt to show that the two phases are reached at the same temperature has been made in [839] using the FESR version of the Weinberg sum rules, which we shall discuss later on, where the constraint has been obtained by assuming that in the QGP phase, the continuum threshold starts from zero. In the QGP phase, the thermodynamics of the plasma is governed by the Stefan–Boltzmann law, as in an ordinary black body transition. This feature has been confirmed by a large number of lattice simulations. The RHIC-BNL heavy ion program is dedicated to the study of transitions to this phase. Actually, the AGS ($2 + 2$ GeV per nucleon in the c.o.m.), CERN-SPS ($10 + 10$ GeV) and RHIC ($100 + 100$ GeV) are expected to reach this phase transition. The phase diagram of QCD is shown in Fig. 57.1 in the T plane versus the baryonic chemical potential μ normalized per quark (not per baryon).

CS2 (two flavours) and CS3 (three flavours) are colour superconducting phases corresponding to large density and low T regions, which are not crossed by the heavy ion collisions but belong to the neutron star physics. The small drop of CS matter is expected to be due to one Cooper pair composed with a (ud scalar diquark) and one massive quark [840]. Some new crystalline phases due to oscillating $\langle \bar{q}q(x) \rangle$ condensates may also appear [841], which may compete with CS2 at $\mu \approx 400$ MeV. Hadronic phase at small value of $(T,\ \mu)$ and the QGP phase at large value of $(T,\ \mu)$ have been known for a long time. However, it is not quite clear if the phase transition line separating them starts at $(T = T_c,\ \mu = 0)$ but at an endpoint E, a remnant of the so-called QCD tricritical point which QCD possesses in the massless quark limit.

https://doi.org/10.1017/9781009290296.071 Published online by Cambridge University Press

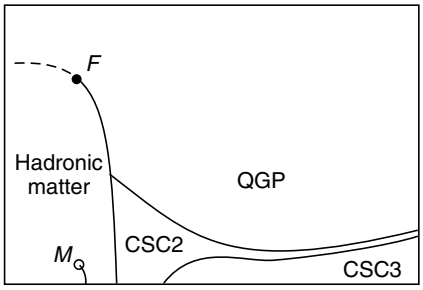

Fig. 57.1. QCD phase diagram.

57.2 Big-bang versus heavy ion collisions

- In both cases, the expansion law is roughly the Hubble law $v(r) \sim r$, but strongly isotropic in the case of the heavy ion collisions.
- The acceleration history is not well measured (for Big Bang, one uses distant supernovae) but both show small dipole components.
- In both cases, the major puzzle is how the large entropy was actually produced, and why it happened so early, with a subsequent expansion close to the adiabatic expansion of equilibrated hot medium.

57.3 Hadronic correlations at finite temperature

The analysis of hadronic correlations at finite temperature is of great interest in connection with the modifications of hadronic properties in hot hadronic matter. The structure of the QCD correlations at intermediate distances also reflects the changes in the interaction between quarks and gluons. In the context of QSSR, this analysis has been extensively studied [839,842–851]. However, further assumptions on the T-behaviour of the condensates or information from some other approaches [852–854] are needed in the analysis as well as some assumptions on the shape of the hadron spectrum, which limit the accuracy of the results. Neverthless, interesting quantitative results can be extracted. We shall be concerned here with the retarted (advanced) correlator (the causal one does not have useful analytic properties [855]) of the hadronic current $J(x)$ (generic notation):

$$\Pi_R(\omega, \mathbf{q}) = i \int d^4x \; e^{iqx} \mathrm{theta}(\mathrm{x}^0) \langle\langle [\mathrm{J(x)}, \mathrm{J}^\dagger(0)] \rangle\rangle \; , \tag{57.1}$$

where $q \equiv (\omega, \mathbf{q})$ and $\langle\langle \ldots \rangle\rangle$ stands for the Gibbs average:

$$\langle\langle \ldots \rangle\rangle = \sum_n W_n \langle n| \ldots |n\rangle \; , \quad W_n \equiv \exp[(\Omega - E'_n)/T] \; . \tag{57.2}$$

$|n\rangle$ is a complete set of the eigenstates of the QCD effective Hamiltonian:

$$H'|n\rangle = E'|n\rangle \; , \quad H = H - \mu N \; , \tag{57.3}$$

where H is the usual Hamiltonian, N is some conserved additive quantum number (baryonic charge, strangeness, ...), μ is the corresponding chemical potential,

https://doi.org/10.1017/9781009290296.071 Published online by Cambridge University Press

and $\Omega = -T \ln Tr \exp(-H'/T)$. The two-point correlator is analytic in the upper half-plane of the complex variable ω and obeys the dispersion relation:

$$\Pi_R(\omega,\ \mathbf{q}) = \int_{-\infty}^{+\infty} \frac{du}{u - \omega - i\epsilon} \rho(u,\ \mathbf{q}) \,. \tag{57.4}$$

The spectral density ρ is:

$$\begin{aligned} \rho(\omega,\ \mathbf{q}) = (2\pi)^3 \sum_{n,m} & \langle n|J|m\rangle\langle m|J|n\rangle \\ & \times W_n[1 - \exp(-\omega/T)]\delta(\omega - \omega_{mn})\delta^{(3)}(\mathbf{q} - \mathbf{k}_{mn}) \,, \end{aligned} \tag{57.5}$$

where:

$$\omega_{mn} = E'_m - E_n \,, \qquad \mathbf{k}_{mn} = \mathbf{k}_m - \mathbf{k}_n \,. \tag{57.6}$$

Noting that in the set of discrete points of the imaginary half-axis, the retarded correlator in Eq. (57.1) coïncides with the corresponding Matsubara Green functions [856]:

$$\Pi_R(i\omega_n) = \mathcal{G}(\omega_n - i\mu) \,, \tag{57.7}$$

where:

$$\omega_n = 2\pi n T \,, \qquad n = 0, 1, 2, \ldots, \tag{57.8}$$

one can then calculate it using Feynmann diagram techniques in the Matsubara representation [856] (imaginary time formalism). [1] For $\omega \to \infty$, the correlator in Eq. (57.1) tends to its perturbative QCD value. Therefore, it is reasonable to use quarks and gluons in Eq. (57.5), in order to get its asymptotic behaviour. Using the OPE, one can add, to the perturbative part, the NP contributions due to the quark and gluon condensates:

$$\Pi_R(q) = \sum_n C_n(q)\langle\langle \mathcal{O}_n \rangle\rangle \,, \tag{57.9}$$

where C_n is the Wilson coefficient obtained at zero temperature. The temperature dependence appears when one takes the Gibbs averages $\langle\langle \ldots \rangle\rangle$ of the local operators $\mathcal{O}_n$. Summing up all contributions from different $\mathcal{O}_n$, one expects to recover the Matsubara results. The radiative corrections appearing in the evaluation of the condensates should be of the form $\alpha_s(\nu)\ln(T/\nu)$ as only T is the dimensional scale in the calculation of condensates at finite T, such that it is important to determine the T value above which one can rely on the calculation. Formally, T should be much bigger than the QCD scale Λ. For the time being, we shall ignore radiative corrections and assume that perturbation theory works for T around 150 MeV.

[1] Real time formalism as discussed in [857] is not convenient for the problem discussed here, where one evaluates the spectral function.

https://doi.org/10.1017/9781009290296.071 Published online by Cambridge University Press

57.4 Asymptotic behaviour of the correlator in hot hadronic matter

Let us consider the correlator associated with the light quark vector current:

$$J_\mu(x) = \bar{\psi}\gamma_\mu\psi \tag{57.10}$$

which has the quantum number of the photon γ. The imaginary part of the correlator defined as in Eq. (57.5) is then the probability of the absorption of a virtual γ-quanta of time-like momenta $\omega^2 - \mathbf{q}^2 > 4m_q^2 (m_q \to 0)$ by the matter. The virtual quanta consisting of free fermions $n_F(E)$ are converted into a quark-antiquark pair at a rate proportional to $[1 - n_F(E_1)][1 - n_F(E_2)]$ according to Pauli's principle where $E_{1,2}$ are the quark energies. At the same time, the γ-quanta are produced with the rate $n_F(E_1)n_F(E_2)$. Therefore, the rate of the disappearance of time-like γ-quanta in the fermionic medium $\rho^g_{\mu\nu}$ is:

$$\rho^g_{\mu\nu}(\omega,\ \mathbf{q}) = \sum_s \int \mathrm{LIPS}(E_1, \mathbf{k_1}, E_2, \mathbf{k_2}) \times \langle 0|J_\mu|\bar{\psi}\psi\rangle\langle\bar{\psi}\psi|J_\nu|0\rangle \left\{[1 - n_F(E_1)][1 - n_F(E_2)] - n_F(E_1)n_F(E_2)\right\} , \tag{57.11}$$

where:

$$\mathrm{LIPS}(E_1, \mathbf{k_1}, E_2, \mathbf{k_2}) \equiv \frac{d^3k_1}{2E_1(2\pi)^3}\frac{d^3k_2}{2E_2(2\pi)^3}\delta(\omega - E_1 - E_2)\delta^{(3)}(\mathbf{q} - \mathbf{k_1} - \mathbf{k_2}) . \tag{57.12}$$

The numbers of fermions and bosons inside the plasma are:

$$n_F(z) = 1/(1 + e^z) , \qquad n_B = 1/(1 - e^z) . \tag{57.13}$$

The γ-virtual space-like quanta ($\omega^2 - \mathbf{q}^2 < 0$) can be absorbed by the (anti) quarks of the medium at a rate, proportional to $n_F(E_1)[1 - n_F(E_2)]$ and emitted at the rate $n_F(E_2)[1 - n_F(E_1)]$: $E_1 = \omega + E_2$. Thus, it disappears at a scattering rate:

$$\rho^s_{\mu\nu}(\omega,\ \mathbf{q}) = \sum_g \int \mathrm{LIPS}(E_1, \mathbf{k_1}, -E_2, -\mathbf{k_2}) \times \langle\psi|J_\mu|\bar{\psi}\rangle\langle\bar{\psi}|J_\nu|\psi\rangle \left\{n_F(E_1)[1 - n_F(E_2)] - n_F(E_2)[1 - n_F(E_1)]\right\} , \tag{57.14}$$

where one can notice that the location of the singularities at $T \neq 0$ differs qualitatively from that at $T = 0$ as shown in Fig. 57.2.

Therefore the spectral function reads:

$$\rho(\omega,\ \mathbf{q}) = \theta(\omega^2 - \mathbf{q}^2 - t_c)\rho^g + \theta(\omega^2 - \mathbf{q}^2)\rho^s , \tag{57.15}$$

where t_c is some threshold and the spectral function does not vanish for both time-like and space-like momenta. ρ^s corresponds to the scattering term which increases with the particle density and appears as we use a mixed state of matter instead of the vacuum, when

https://doi.org/10.1017/9781009290296.071 Published online by Cambridge University Press

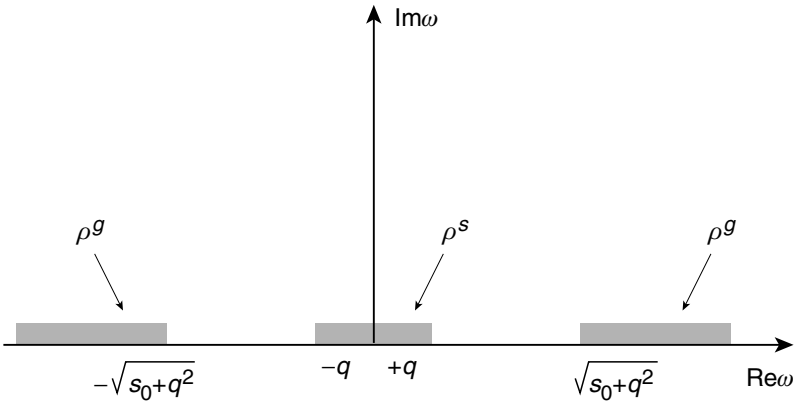

Fig. 57.2. Location of singularities in the complex ω plane.

averaging the initial commutator. At $T \neq 0$, the correlator of the vector isovector current:

$$J_\mu = \frac{1}{2}(\bar{u}\gamma_\mu u - \bar{d}\gamma_\mu d) \,, \tag{57.16}$$

contains two invariants Π_T and Π_L, which, in the rest frame of matter, can be defined as follows:

$$\Pi_{00} = \mathbf{q}^2 \Pi_L \,, \qquad \Pi_{ij} = \left(\delta_{ij} - \frac{q_i q_j}{\mathbf{q}^2}\right) \Pi_T + \frac{q_i q_j}{\mathbf{q}^2} \omega^2 \Pi_L \,. \tag{57.17}$$

Using Eqs. (57.11) to (57.14), one can deduce Im $\Pi_{L,T}$. To lowest order in α_s, the Euclidian asymptotic of the form factors reads [842]:

$$\begin{aligned}
\rho_L^g &= \frac{3}{32\pi^2} \int_{-v}^{+v} dx \; (1-x^2) \, \mathrm{th}(q^+/2T) \,, \\
\rho_L^s &= \frac{3}{32\pi^2} \int_{-v}^{+v} (1-x^2)[2n_F(q^+/2T) - 2n_F(q^-/2T)] \,, \\
\rho_T^g &= \frac{3}{64\pi^2}(\omega^2 - q^2) \int_{-v}^{+v} dx \; (2 + x^2 - v^2) \, \mathrm{th}(q^+/4T) \,, \\
\rho_T^s &= \frac{3}{64\pi^2}(\omega^2 - q^2) \int_{-v}^{+v} dx \; (2 + x^2 - v^2) \, [2n_F(q^+/2T) - 2n_F(q^-/2T)] \,,
\end{aligned} \tag{57.18}$$

where: $q^+ \equiv qx + \omega$; $q^- \equiv qx - \omega$ and:

$$v = \sqrt{1 - \frac{4m_q^2}{(\omega^2 - \mathbf{q}^2)}} \,. \tag{57.19}$$

In the case of a resonance at rest with respect to the medium ($\mathbf{q} \to 0$), one knows that the two previous form factors are proportional to each other [858]:

$$\Pi_T(\mathbf{q} = 0) = (\omega^2 - \mathbf{q}^2)\Pi_L|_{\mathbf{q}=0} \,. \tag{57.20}$$

https://doi.org/10.1017/9781009290296.071 Published online by Cambridge University Press

Therefore, considering the longitudinal form factor, one has:

$$\rho_L^g(\mathbf{q}=0,\ \omega) = \mathrm{th}\big(\omega^2 - 4m_q^2\big)\mathrm{th}(\omega/4T)\rho^0(\omega^2)\ ,$$
$$\rho_L^s(\mathbf{q}=0,\ \omega) = \delta(\omega^2)\int_{4m_q^2}^{\infty} du^2 2n_F(u/2T)\rho^0(u^2)\ , \tag{57.21}$$

with:

$$\rho^0(\omega^2) = \frac{3}{16\pi^2}v(3-v^2)\ ,\quad v = \sqrt{1-\frac{4m_q^2}{\omega^2}}\ , \tag{57.22}$$

where the term ρ^s is due to the scattering with matter and vanishes for $T=0$.

Systematic expansion of the spectral function can be done using the so-called *hard thermal loop expansion* [859], where the order parameters are the 'hard scale' of the order of T or larger and the 'soft scale' of the order of gT (g being the QCD coupling, which is assumed to be small), where, at this soft scale, collective effects in the plasma lead to effective (resummed) propagators and vertices parametrizing the modification of the physics at this scale, which one can formulate using an effective Lagrangian [860].

To one loop, the vector spectral function behaves as [861]:

$$\rho^g(\omega,\mathbf{q}) \sim \alpha_s T^2\left[\ln\left(\frac{\omega T}{m^2}\right) + \text{constant}\right] \tag{57.23}$$

where $m^2 \sim \alpha_s T^2$ is related to the quark thermal mass. Therefore, the large $\ln(1/\alpha_s)$ dominates over the constant term. However, the two-loop contribution is of the same order as the one-loop graph due to the enhancement factor $1/m^2 \sim 1/\alpha_s$ which compensates the α_s factor associated to the quark-gluon coupling from the gluon exchange. This $1/m^2$ factor originates from the presence of collinear singularities. This result questions the validity of the QCD perturbative calculation in this regime. Phenomenological applications of these results to the the lepton pair production in the quark-gluon plasma are discussed in [861].

57.5 Quark condensate at finite T

The temperature dependence of the $\langle\bar\psi\psi\rangle$ quark condensate can be expressed as:

$$\langle\langle\bar\psi\psi\rangle\rangle = \frac{Tr\left(\bar\psi\psi\exp -H/T\right)}{Tr\left(\exp -H/T\right)}\ . \tag{57.24}$$

It has been studied in [852] using an effective Lagrangian approach, where one has exploited the fact that, at low temperatures, the behaviour of the partition function is dominated by the contributions from the lightest particles occuring in the spectrum. In QCD, this lightest particle is the pion, which is massless in the chiral limit. Interaction among the pions generates power corrections controlled by the expansion parameter $T^2/8f_\pi^2$, while the contribution due to a massive state i is suppressed as $\exp(-M_i/T)$, where M_i is the corresponding hadron mass. At low temperature, one can express the pressure as the

https://doi.org/10.1017/9781009290296.071 Published online by Cambridge University Press

temperature-dependent part of the free energy density:

$$P = E_0 - Z \,, \tag{57.25}$$

where E_0 is the vacuum energy density and Z is the partition function:

$$Z = -T \lim_{L\to\infty} L^{-3} \ln[Tr \exp(-H/T)] \,. \tag{57.26}$$

The quark condensate is given by the *log*-derivative of the partition function with respect to the quark mass:

$$\langle\langle \bar{\psi}\psi \rangle\rangle = \frac{\partial Z}{\partial m} \,, \tag{57.27}$$

where at zero temperature:

$$\langle \bar{\psi}\psi \rangle = \frac{\partial E_0}{\partial m} \,. \tag{57.28}$$

Therefore, at finite temperature:

$$\langle\langle \bar{\psi}\psi \rangle\rangle = \langle \bar{\psi}\psi \rangle \left(1 + \frac{c}{F^2} \frac{\partial P}{\partial m_\pi^2}\right) \,, \tag{57.29}$$

where:

$$c \simeq 0.90 \pm 0.15 \tag{57.30}$$

is a constant ($c = 1$ in the massless case) fixed from π-π scattering data, while $F = 88$ MeV is the value of the pion decay constant in the chiral limit ($f_\pi = 92.4$ MeV). In the massless limit:

$$P = \frac{\pi^2}{30} T^2 \left(1 + \frac{16}{9} x_T^2 \ln \frac{\Lambda_q}{T} + \mathcal{O}(T^6)\right) \,. \tag{57.31}$$

The log-scale is related to the p^4-term of the effective Lagrangian and is fixed from π-π scattering analysis to be:

$$\Lambda_q \simeq (470 \pm 110) \text{ MeV} \,. \tag{57.32}$$

To order T^8, the temperature dependence of the condensate in the chiral limit reads:

$$\langle\langle \bar{\psi}\psi \rangle\rangle = \langle \bar{\psi}\psi \rangle \left(1 - x_T - \frac{1}{6} x_T^2 - \frac{16}{9} x_T^3 \ln \frac{\Lambda_q}{T} + \mathcal{O}(T^8)\right) \,, \tag{57.33}$$

where:

$$x_T = \frac{T^2}{8F^2} \,, \tag{57.34}$$

indicating that the temperature scale is set by $\sqrt{8}F \simeq 250$ MeV. The behaviour of the condensate versus T is given in Fig. 57.3 for massless quarks. One can deduce that the condensate gradually melts for increasing T, and vanishes for massless quarks at $T_c \approx 190$ MeV, indicating the occurence of a phase transition at this temperature.

https://doi.org/10.1017/9781009290296.071 Published online by Cambridge University Press

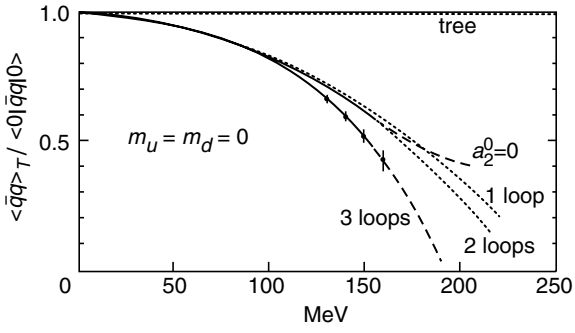

Fig. 57.3. T-behaviour of the quark condensate in the chiral limit from [852]. Here and in the following $\langle\bar{q}q\rangle \equiv \langle\bar{\psi}\psi\rangle$.

The inclusion of the quark masses can be obtained on the basis of Eq. 57.29. It is shown that the effect shifts the value of T_c to higher value of about 240 MeV.

Using a dilute gas approximation (i.e. neglecting the self-interactions of hadrons, as they manifest as the product of their density $n_i n_j \sim \exp[-(M_i + M_j)/T]$) in the low-temperature region, the effect of massive states induces a positive correction of order T^2 to the condensate:

$$\Delta\langle\bar{\psi}\psi\rangle \simeq -\langle\bar{\psi}\psi\rangle \frac{T^2}{F^2} \sum_i h_1\left(\frac{T}{M_i}\right) \frac{m}{m_\pi^2} M_i \frac{\partial M_i}{\partial m} \ , \tag{57.35}$$

with:

$$h_1(\tau) \equiv \frac{1}{2\pi^2\tau^2} \int_0^\infty dx \ \mathrm{sh}^2 x [\exp(\mathrm{ch}x/\tau) - 1]^{-1} \ , \tag{57.36}$$

and:

$$\frac{\partial M_i}{\partial m} = \frac{1}{2M_i} \langle p_i|\bar{\psi}\psi|p_i\rangle \ , \tag{57.37}$$

where $|p_i\rangle$ denotes a one-particle state of momentum p. Therefore, Eq. (57.37) counts the number of valence quarks of type u and d inside the hadrons. One can estimate the uncertainties in this approximation by considering the kaon mass formula:

$$M_K^2 = (m + m_s)B \ , \tag{57.38}$$

from which one can deduce:

$$m\frac{\partial M_K}{\partial m} = \frac{m}{2(m + m_s)} M_K[1 + \text{corrections}] \ . \tag{57.39}$$

A comparison of the numerical value from Eqs. (57.37) and (57.39) show that the naïve relation in Eq. (57.37) underestimates the real value by a factor about 1.4. The effect of massive states is such that it accelerates the melting of the condensate and implies a fast drop until the phase transition of about 200 MeV. We show in Figs. 57.4 and 57.5, the sum

https://doi.org/10.1017/9781009290296.071 Published online by Cambridge University Press

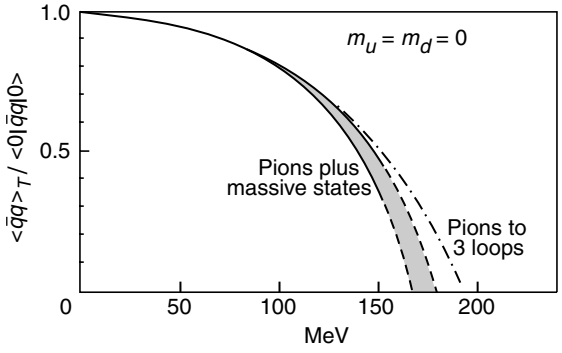

Fig. 57.4. T-behaviour of the quark condensate in the chiral limit including massive states.

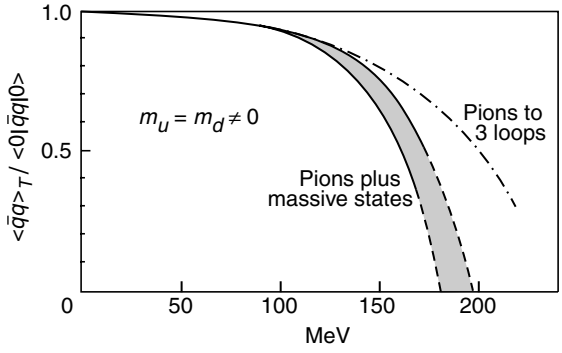

Fig. 57.5. T-behaviour of the quark condensate in the massive quark limit including massive states.

of the different effects in the case of massless and massive quarks. The uncertainties in evaluating the quantity in Eq. (57.37) are given by the shaded region in Figs. 57.4 and 57.5.

One can deduce that the critical temperature is:

$$\begin{aligned} T_c &\simeq 170 \text{ MeV} \qquad (m_u = m_d = 0) \\ &\quad 190 \text{ MeV} \qquad (m_u, m_d \neq 0) \, . \end{aligned} \tag{57.40}$$

Such a value of T_c has been confirmed by lattice simulation with two dynamical Kogut–Susskind fermions [862]:

$$T_c(n_f = 2) \simeq 150 \text{ MeV} \, , \tag{57.41}$$

and by instanton liquid model [386]. In the case of the $\langle \bar{s}s \rangle$, the m_s corrections shifts T_c to higher values of about 250 MeV [863]. Similar analysis can be done respectively for the entropy density S, energy density U and heat capacity C_v:

$$S = \frac{\partial P}{\partial T} \, , \qquad U = TS - P \, , \qquad C_v = \frac{\partial U}{\partial T} = T \frac{\partial S}{\partial T} \, , \tag{57.42}$$

where for massless quarks, P is given in Eq. (57.31).

https://doi.org/10.1017/9781009290296.071 Published online by Cambridge University Press

57.6 f_π at finite temperature

In [853], the T dependence of the pion decay constant has been also studied within the composite model framework. It has been found that:

$$\frac{f_\pi^2(T)}{f_\pi^2(0)} \simeq \frac{\langle\langle\bar{\psi}\psi\rangle\rangle}{\langle\bar{\psi}\psi\rangle} \,. \tag{57.43}$$

Near the critical temperature, the relation [839]:

$$\frac{f_\pi(T)}{f_\pi(0)} \simeq (3.0 \sim 3.2)\left(1 - \frac{T}{T_c}\right)^{1/2} \,, \tag{57.44}$$

might be more accurate than the one derived from Eq. (57.33) in the chiral limit.

57.7 Gluon condensate

Using naïve dimensional counting, it has been argued in [842] that the perturbative contribution to the Gibbs average of the gluon condensate is of the form:

$$\langle\langle G^2\rangle\rangle \sim \langle G^2\rangle + cT^4\alpha_s(T) \,, \tag{57.45}$$

such that this pertubative contribution is negligible. Using a more involved estimate, they relate this temperature effect to the trace of the gluonic part of the energy momentum tensor sandwiched between two pion states:

$$\langle\langle G^2\rangle\rangle \sim \langle G^2\rangle + F(m_\pi,\ T)\langle\pi|G^2|\pi\rangle \,, \tag{57.46}$$

where F is a function that is dependent on m_π and T. An explicit evaluation gives [854]:

$$\langle\langle G^2\rangle\rangle \sim \langle G^2\rangle - \pi^3\frac{16384}{3465}n_f^2\left(n_f^2-1\right)x_T^4\left(\ln\frac{\Lambda_q}{T} - \frac{1}{4}\right) \,, \tag{57.47}$$

where the temperature-dependent term is a very small correction, although showing that the gluon condensate melts very smoothly for increasing temperature.

57.8 Four-quark condensate

The temperature dependence of the four-quark condensate has been often estimated using the vacuum saturation assumption:

$$\langle\langle\mathcal{O}_4\rangle\rangle \equiv \langle\langle\bar{\psi}\Gamma_1\psi\bar{\psi}\Gamma_2\psi\rangle\rangle \sim \langle\langle\psi\rangle\rangle^2 \,, \tag{57.48}$$

which should only be taken very qualitatively, as there are evidences that, already at zero temperature, the vacuum saturation assumption is violated by a factor of 2 to 3 (see previous

https://doi.org/10.1017/9781009290296.071 Published online by Cambridge University Press

sections). In [848], the temperature dependence of the four-quark operators in different channels has been studied within the sum rule itself, where the approximate behaviour:

$$\langle\langle \mathcal{O}_4 \rangle\rangle \approx \langle \mathcal{O}_4 \rangle \left[1 - \frac{T^2}{(330 \text{ MeV})^2} \right] , \tag{57.49}$$

has been obtained to be compared with that:

$$\langle\langle \mathcal{O}_4 \rangle\rangle \sim \langle \bar{\psi}\psi \rangle^2 \left[1 - \frac{T^2}{(177 \text{ MeV})^2} \right] , \tag{57.50}$$

which one would have obtained if the vacuum saturation for the four-quark condensate has been used together with the previous T-dependence of $\langle \bar{\psi}\psi \rangle$. The smooth dependence of the four-quark dependence can be qualitatevely understood when using the fact that at the optimization scale of the LSR, one has the relation:

$$M_\rho \sim \langle\langle \alpha_s \mathcal{O}_4 \rangle\rangle^{1/6} , \tag{57.51}$$

and as one will see later on, the ρ-meson mass varies smoothly with temperature below T_c.

57.9 The ρ-meson spectrum in hot hadronic matter

The ρ meson mass spectrum was originally studied in [842] using Laplace transform sum rules. The ρ coupling to the longitudinal part of the spectral function is introduced as:

$$\rho_l = \frac{M_\rho^2}{2\tilde{\gamma}_\rho^2} \delta\left(\omega^2 - \mathbf{q}^2 - m_l^2\right) . \tag{57.52}$$

The LSR reads:

$$\begin{aligned} \mathcal{F}(\tau) &\simeq 4\pi^2 \frac{M_\rho^2}{2\tilde{\gamma}_\rho^2} \exp\left(- M_\rho^2 \tau \right) \\ &= \int_0^{t_c} dt \ \exp(-t\tau) \text{th}(\sqrt{t}/4T) \\ &\quad + 2 \int_0^\infty dt \ [n_f(\sqrt{t}/2T) - \frac{1}{3} n_f(\sqrt{t}/2T)] \\ &\quad + \frac{\pi}{3} \langle \alpha_s G^2 \rangle \tau - 2\pi^3 \alpha_s \langle \bar{\psi}\psi \rangle^2 \tau^2 . \end{aligned} \tag{57.53}$$

Instead, we work with moments:

$$\mathcal{R}(\tau) \equiv - \frac{d}{d\tau} \ln \mathcal{F}(\tau) , \tag{57.54}$$

which is convenient for studying the spectrum as it free from the unknown longitudinal coupling $\tilde{\gamma}_\rho$. In addition, width corrections which might be large here partially cancel in the ratio. Stability of the LSR moments versus the usual parameters (τ, t_c) has been studied in

https://doi.org/10.1017/9781009290296.071 Published online by Cambridge University Press

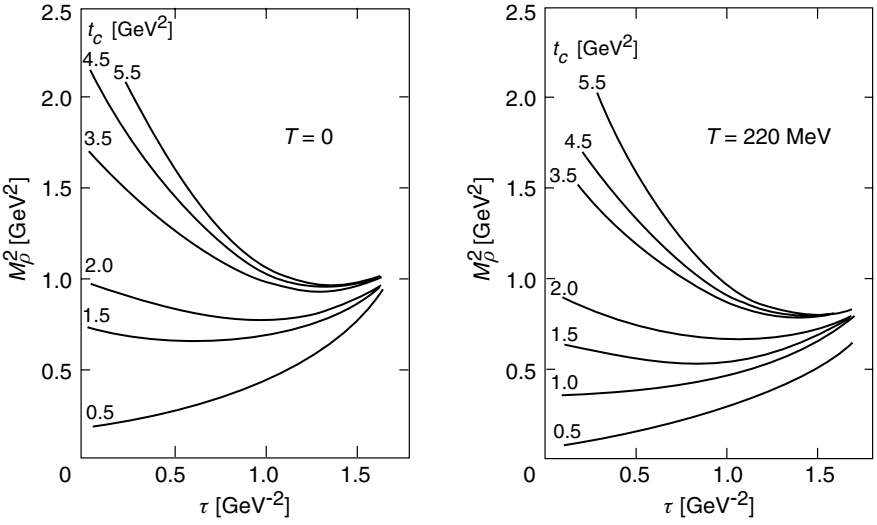

Fig. 57.6. τ and t_c stabilities analysis of the rho meson mass.

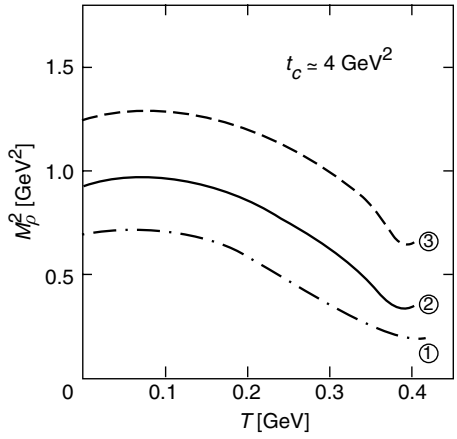

Fig. 57.7. T-behaviour of the rho meson spectrum.

detail in [843] using different values of the QCD input parameters, where, in the analysis, the small variations of the gluon and four-quark condensates with temperature have been neglected. This analysis is shown in Fig. 57.6.

The optimal result of the ρ-meson mass from [843] is shown in Fig. 57.7, where the smooth T-dependence decrease of the spectrum differs from the sharp change at T_c obtained from [842]. This difference is understood to be due to the effect of the change of the continuum threshold from 0.8 to 1.5 GeV^2 with T in [842], where stability in the variable τ of the LSR has not yet been reached. This result also differs from the expectation [864] that $M_\rho(T) > M_\rho(0)$. We conclude from this figure that the hot fermi gas does not lead to a

https://doi.org/10.1017/9781009290296.071 Published online by Cambridge University Press

drastic change of the spectra in the region below 200 MeV. Such behaviour just indicates that the ρ-meson mass at zero and at $T \leq T_c$ has qualitatively the same feature, and a posteriori indicates that the quark hadron duality used at zero temperature is also applicable here. This feature just indicates that some criticisms [847] on the non-validity of the quark-gluon basis at small T in Eq. (57.2) are obviously wrong, as in this region the quark-hadron duality is expected to work better. In the same way, some other arguments raised by [847] like the non-consideration of non-peturbative effects (confinement) within the approach of [842] reviewed here are not at all justified, as has been demonstrated in the analysis of the exactly solvable QCD-like two-dimensional sigma $O(N)$ and Schwinger models [846]. The analysis of [843] has been completed by giving sets of FESR:

$$
\begin{aligned}
4\pi^2 \frac{M_\rho^2}{\tilde{\gamma}_\rho^2} &\simeq \int_0^{t_c} dt\ \mathrm{th}(\sqrt{\mathrm{t}}/4\mathrm{T}) + 2\int_0^{\infty} \mathrm{dt}\ \left(\mathrm{n_F} - \frac{1}{3}\mathrm{n_B}\right) \\
4\pi^2 \frac{M_\rho^4}{\tilde{\gamma}_\rho^2} &\simeq \int_0^{t_c} dt\ t\ \mathrm{th}(\sqrt{\mathrm{t}}/4\mathrm{T}) - \frac{1}{3}\pi\langle\alpha_\mathrm{s}\mathrm{G}^2\rangle \\
4\pi^2 \frac{M_\rho^6}{\tilde{\gamma}_\rho^2} &\simeq \int_0^{t_c} dt\ t^2\ \mathrm{th}(\sqrt{\mathrm{t}}/4\mathrm{T}) - \frac{896}{81}\pi^3\alpha_\mathrm{s}\langle\bar{\psi}\psi\rangle^2\ ,
\end{aligned}
\tag{57.55}
$$

that are necessary for checking the consistency of the parameters obtained from the LSR. However, one should understand that the accuracy of the constraints decreases with increasing dimensions. These FESR have been used in [845] for studying the T dependence of the continuum threshold t_c, a result which has been confirmed by [839] within the framework of composite models. Namely a smooth dependence with T has been found:

$$
\frac{t_c(T)}{t_c(0)} \simeq \frac{f_\pi(T)}{f_\pi(0)}\ . \tag{57.56}
$$

57.10 ρ-meson coupling and width

The T dependence of the ρ meson coupling has been also studied in [849] in which a smooth dependence was found as well:

$$
\frac{1}{\tilde{\gamma}_\rho(T)} \simeq \frac{1}{\tilde{\gamma}_\rho(0)}\left(1 - \frac{2}{3}x_T + \cdots\right)\ . \tag{57.57}
$$

These smooth dependences of the rho-meson mass and coupling were confirmed later in [850].

The T-dependence of the ρ-meson width has been proposed in [865] by using the relation between the $\rho\pi\pi$ coupling and f_π through the KSFR relation (see Part I):

$$
g_{\rho\pi\pi} = \frac{M_\rho}{\sqrt{2}f_\pi}\ , \tag{57.58}
$$

https://doi.org/10.1017/9781009290296.071 Published online by Cambridge University Press

and its relation to the $\rho \to \pi\pi$ width:

$$\Gamma_{\rho\to\pi\pi} = \frac{g^2_{\rho\pi\pi}}{4\pi}\frac{M_\rho}{12}\,, \tag{57.59}$$

from which, it is easy to deduce the desired T-dependence:

$$\Gamma_\rho(T) \simeq \Gamma_\rho(0)\left(1 - \frac{T^2}{4f_\pi^2}\right)^{-1}\,, \tag{57.60}$$

showing that for increasing T-values, the ρ-meson becomes broader and difficult to assign as a *true* resonance. This result has been confirmed from a recent study of the T-dependence of the imaginary part of the ρ-meson propagator [866].

Therefore, one can conclude from our previous analysis that the ρ-meson mass is almost insensitive to the T-variation, while its non-identification as a resonance is mainly due to the large increase of its hadronic $\pi\pi$ width at non-zero temperature. As a result, the study of dilepton-invariant mass in nuclear collisions through Drell–Yan processes at the rho-meson mass energy will not reveal a clear resonance structure.

57.11 Deconfinement phase and chiral symmetry restoration

We mentioned in the introduction that the Weinberg sum rules have been used in [839] for studying the relation between the deconfinement temperature T_d and the chiral symmetry restoration temperature T_c. At finite temperature the first Weinberg sum rule reads [845]:

$$8\pi^2 f_\pi^2(T) \simeq \int_0^{t_c(T)} d\omega^2\, \text{th}(\omega/4T) + 2\int_0^\infty d\omega^2\, n_F(\omega/2T)\,, \tag{57.61}$$

where t_c is the continuum threshold separating the hadron from the continuum. Assuming that in the QGP, $t_c(T_d) = 0$, one can derive the constraint [839]:

$$f_\pi(T_d) = \frac{T_c}{\sqrt{6}}\left(\frac{T_d}{T_c}\right)\,, \tag{57.62}$$

relating the chiral restoration temperature T_c with the deconfinement one T_d. The graphical resolution of the previous equality is obtained for:

$$T_d \approx T_c\,, \tag{57.63}$$

showing that the chiral restoration and the deconfinement phase are obtained at about the same temperature.

57.12 Hadronic couplings

The extension of the present framework for evaluating the meson trilinear couplings has been done in [845] using the symmetric point configuration of the vertex firstly proposed in [636,637]. It has been found that the couplings vanish like f_π^n, where n is a positive

https://doi.org/10.1017/9781009290296.071 Published online by Cambridge University Press

model-dependent number, showing that hadrons decouple in the deconfinement phase. It is also remarkable to notice that the $\pi^0\gamma\gamma$ coupling vanishes at high temperature indicating the absence of the QED anomaly in the QGP phase. This result has been confirmed by some field theory model calculation [867].

57.13 Nucleon sum rules and neutron electric dipole moment

The extension of the previous application for studying the nucleon sum rule is straightforward. Noting (see previous section) that:

$$M_N \sim \langle\bar{\psi}\psi\rangle\tau \tag{57.64}$$

where τ is the sum rule scale variable, one also expects that its T-dependence is similar to that of $\langle\psi\psi\rangle$. Finally, nucleon sum rules have been also used in [851] for studying the T-dependence of the ratio of the neutron electric dipole moment over the QCD-θ angle responsible for the strong CP problem, where a smooth variation with temperature has been obtained.

https://doi.org/10.1017/9781009290296.071 Published online by Cambridge University Press